Quinone Methide Precursors as Potential Therapeutics Towards the Realkylation of Aged Acetylcholinesterase

Research Thesis

Presented in Partial Fulfillment of the Requirements for graduation *with research distinction* in the undergraduate colleges of The Ohio State University

by

Travis Glenn Blanton

The Ohio State University
April 2015

Project Advisors: Dr. Ryan J. Yoder and Dr. Christopher S. Callam
Department of Chemistry and Biochemistry

Abstract

Acetylcholinesterase (AChE) is an essential enzyme required by the human body. It hydrolyzes the neurotransmitter acetylcholine (ACh) into two products, choline and acetate, at neurosynaptic junctions. Organophosphorous (OP) nerve agents such as sarin, tabun, and VX are covalent inhibitors of AChE. After a period of time that varies with each OP compound, the inhibition of AChE becomes irreversible due to aging, which is when a de-alkylation of the OP compound in the AChE active site occurs. This aging process results in ACh accumulation in the peripheral and central nervous system. While current pharmaceuticals containing an oxime functional are used to reverse inhibition of AChE by OP compounds, they are not effective in reversing inhibition of AChE after the OP compound has aged. A lack of pharmaceuticals to reverse this pathological aged state was the subject of intense research in the early 1970s, but quickly came to a halt due to the limitations of technology during that era. Now, with far more powerful technology and computational algorithms, research into drug discovery to reactivate aged AChE can be more efficient and effective. The focus of our research is to reactivate aged AChE. Previous reports from the literature demonstrated the capability of Quinone Methides (QMs) to alkylate phosphodiesters and other biological molecules. As a result, this class of compounds has the potential to reverse the aging process and restore function to aged AChE by alkylating the phosphonylated Serine-203 residue in the aged AChE active site. Using the computational methods of Molecular Docking and Molecular Dynamics, a library of Quinone Methide Precursors (QMPs) were tested and evaluated to determine which compounds from the library spent the most time in the aged AChE active site. Additionally, other residues of interest in the active site were examined with the goal of steering design efforts to produce QMPs that have a higher likelihood of potential alkylation.

Acknowledgements

Throughout my time spent at Ohio State, I have met many individuals who have influenced the course of my life significantly enough to warrant mention in this section. Unfortunately only a few will be mentioned; however, I extend my gratitude and appreciation to all – listed or unlisted.

Firstly, I would like to extend my gratitude to Dr. Jeffery Turner for instilling a love of chemistry into a highly impressionable twenty-something. As a result of his influence, I explored research opportunities in the field of organic chemistry and found an opening with a new tenure-track faculty member…

Who happened to be Dr. Ryan J. Yoder, my current research advisor. I would like to thank Ryan for imparting some of his computational chemistry knowledge onto me, as well as for going above and beyond the call of an advisor. Many times, adversity strikes when one is on the cusp of achieving something great. To Ryan, this adversity was always an indication to overcome and advance through in order to reap the rewards that often lie on the other side of struggle. For that, a debt of gratitude is owed. Thank you for believing in me.

I would also like to thank Dr. Christopher Callam for his support, guidance, sharp wit, and excellent sense of humor. Never doubt the power of a good joke (or five.)

I must also thank Dr. Christopher Hadad for using the depth and breadth of his knowledge to help drive the project forward at critical crossroads. Without him, I feel that this thesis may never have been conceptualized. For that, I thank you greatly.

I find it necessary to thank The Ohio State University at Marion for providing the opportunities to explore a breadth of subjects and meet the faculty who teach them. Providing those opportunities allowed me to meet and learn from the following staff and faculty who have forever positively impacted my life: Dr. John Emens, Dr. Robert Klips, Dr. Gary Maul, Professor Emeritus Dr. Brian McEnnis, Dr. Donna Bobbitt-Zeher, Dr. John Maharry Dr. Zakaria Nyongesa, Dr. Chris and Amy

Friesen, Dr. Ben McCorkle, Dr. Terry Pettijohn, Dr. Daniel Wojta, Dr. Christopher Daddis, Dr. Nikole Huffman, Leslie Beary, Lynda Behan, and the staff of Maynard Hall. Sometimes, pleasant conversation and smiling faces are what will take you the distance. Thank you for everything.

Lastly, I would like to thank my friends, family, and those I care deeply about for supporting me during my time as an undergraduate and throughout the medical school application process.

List of Figures

List of Tables

Table Page

Table of Contents

1. Introduction

1.1 OP Exposure and the Role of Quinone Methides as Potential Therapeutic Agents

Organophosphorus compounds (OPs) are a class of compounds that contain a phosphoryl group. Their origin lies in the development of pesticides, when tabun was accidentally discovered by Dr. Gerhard Schrader in Germany in 1936.[1] This extreme toxicity to human life did not go unnoticed, leading to tabun's development into a potential chemical weapon.[2] Since then, many more OP compounds have been created. Of these, the most frequently recognized compounds are sarin (GB), soman (GD), and VX (Figure 1.1).

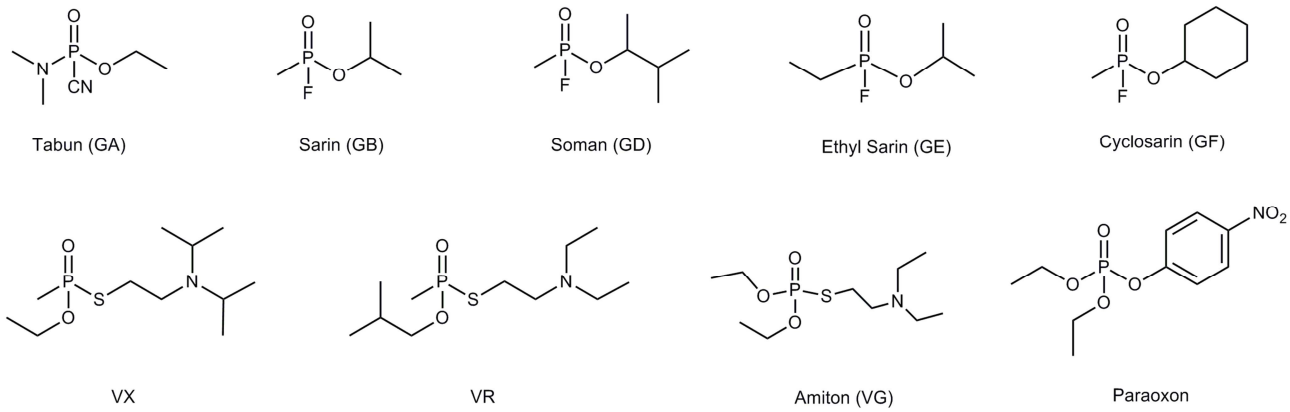

Figure 1.1: Structures of OPs used as chemical warfare agents along with less toxic pesticides, amiton and paraoxon.

In recent history, these OP compounds have been used on military and civilian populations in several countries. Between the months of April and July 1988, the Iraqi army led by Saddam Hussein launched several rockets containing OP nerve agent near the towns of al-Faw, Mehran, and Dehloran in Iraq, killing hundreds to thousands of Iranian solders.[3] In 1995, sarin gas was released into the Japanese subway system by Aum Shinrikyo, a terrorist organization. At least 7 people died and thousands more were hospitalized by the exposure.[4] On

August 21st 2013, the Syrian government launched rockets with sarin-containing warheads into suburbs of Damascus.[5] While there is no official death toll, Médecins Sans Frontières (Doctors Without Borders) has said that at least 3,600 civilians were treated for symptoms consistent with sarin poisoning - vomiting, respiratory issues, and kidney failure at the area's three hospitals within 3 hours of the attack.[6] Records collected by Human Rights Watch show that 734 civilians in the suburb of Zamalka died as a result of the sarin gas attacks, with most victims being children.[7] With casualties primarily being civilians, there has never been a greater need to develop treatments for OP exposure.

OP nerve agents are neurotoxins that are extremely potent. They owe their biological activity to their ability to inactivate the catalytic triad found in acetylcholinesterase (AChE), an enzyme that hydrolyzes the excitatory neurotransmitter acetylcholine. This catalytic triad consists of Ser-His-Glu residues found in the active site. The serine residue of this triad is modified by OPs after they covalently bind to it, effectively inhibiting the enzyme's function. At this time, the treatment protocol for OP exposure is the concurrent administration of 2-Pralidoxime (2-PAM), atropine, and diazepam (Valium) to exposed individuals. 2-Pralidoxime (2-PAM) is a strong nucleophile capable of displacing the OP moiety from the OP-AChE complex. It is the powerhouse of this protocol that restores catalytic function to the inhibited enzyme. If untreated, the OP-AChE complex can undergo a process called aging, where the OP compound is dealkylated.[8] This aging process leaves only the OP's phosphate group attached to the serine residue, irreversibly inhibiting the AChE enzyme (Figure 1.2). The speed at which aging occurs depends solely on the OP compound being used[9]; regardless, the outcome of aging is irreversible inhibition of AChE. After aging occurs, there are no pharmaceuticals currently in

existence that are capable of displacing the OP moiety. The lack of therapeutic agents to reverse the dealkylation of aged AChE is the focus of our research.

Quinone Methides (QMs) are high-energy electrophiles that are used in important biological processes, like lignin biosynthesis in plants, DNA alkylation, and cross-linking of structural proteins.[10,11] The motivation to explore this class of compounds towards reversing the aging process of OP-inhibited AChE comes from two studies. The first, a study from Modica et al.[12], determined that QMPs had the ability to alkylate many nucleophiles, specifically amino acids. The second study, from Bakke et al.[13] reported that QMPs can re-alkylate phosphodiesters in aqueous conditions. The ability of QMP compounds to re-alkylate phosphodiesters and amino acids encourages us in the pursuit of these compounds as a solution to reversing aged AChE, because the OP compounds inhibiting AChE form a phosphodiester bond with the serine residue which results in the OP-AChE complex.

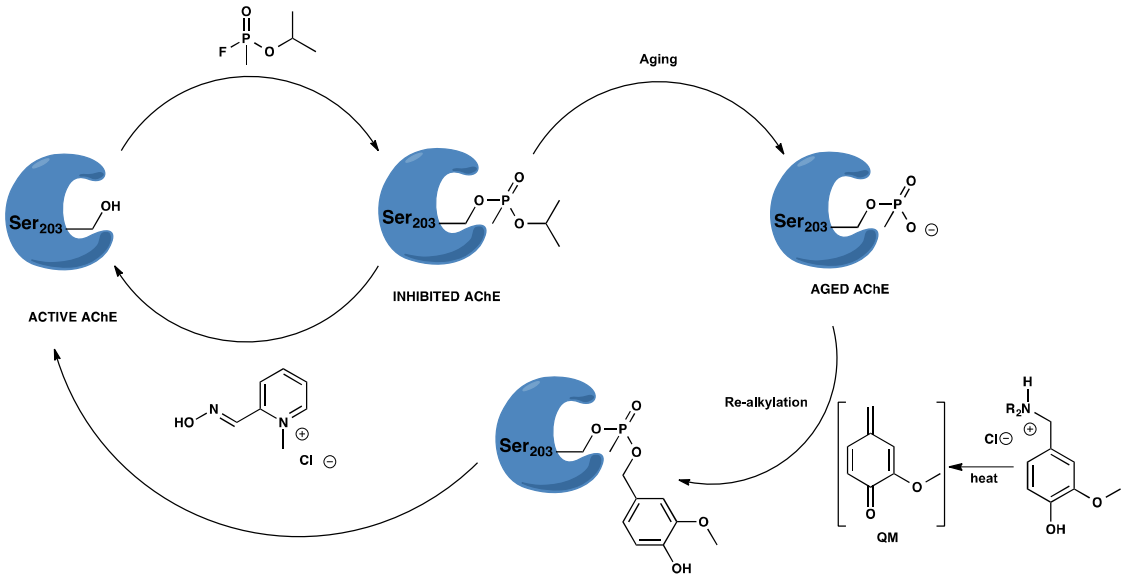

Figure 1.2: The use of QMPs to reactivate aged AChE in order to reverse the aging process of the enzyme upon exposure to nerve agents.

Due to the sheer number of QMPs that could be created, a high-throughput process was required to narrow down the potential candidates for laboratory testing. As a result, computational methods were employed to guide synthetic efforts to produce a QMP that was selective and specific for the active site of AChE.

1.2 References

1. Ballantyne, B. and Marrs, T. C. (1992). Overview of the biological and clinical aspects of organophosphates and carbamates, in Clinical and Experimental Toxicology of Organophosphates and Carbamates, Ballantyne, B. and Marrs, T. C., Eds., Butterworth, Oxford, England, 1.

2. Dacre, J. C. (1984). Toxicology of some Anticholinesterases used as chemical warfare agents - a review, in Cholinesterases, Fundamental and Applied Aspects, Brzin, M., Barnard, E. A. and Sket, D., Eds., de Gruyter, Berlin, Germany, 415.

3. Human Rights Watch, *Iraq's Crime Of Genocide: The Anfal Campaign against the Kurds* (Human Rights Watch, 1994), http://www.hrw.org/reports/1994/05/01/iraq-s-crime-genocide-anfal-campaign-against-kurds.

4. Seto, Dr. Yasuo: The Sarin Gas Attack in Japan and the Related Forensic Investigation. *Org. for Prohibition of Chemical Weapons*, June 2001, http://www.opcw.org/news/article/the-sarin-gas-attack-in-japan-and-the-related-forensic-investigation/ (accessed September 16th, 2014)

5. Rogin, J. Exclusive: U.S. to Bring Chemical Weapons Witnesses Out of Syria. *The Daily Beast*, May 2013, http://www.thedailybeast.com/articles/2013/05/22/exclusive-u-s-to-bring-chemical-weapons-witnesses-out-of-syria.html (accessed May 27, 2013)

6. Médecins Sans Frontières, "Syria: Thousands Suffering from Neurotoxic Symptoms Treated in Hospitals Supported by MSF," August 24, 2013.

7. Human Rights Watch, *Attacks on Ghouta*.(Human Rights Watch, 2013), http://www.hrw.org/node/118724/section/4 http://www.hrw.org/reports/1993/iraqanfal/.

8. Michel, H. O., Hackley B. E. Jr, Berkowitz, L., List, G., Hackley, E. B., Gilliam, W. and Paukan, M. (1967) Aging and dealkylation of soman (pinocolylmethyl- phosphonofluoridate)-inactivated eel cholinesterase. Arch. Biochem. Biophys. 121, 29–34.

9. Worek, F., Szinicz, L., Eyer, P. and Thiermann, H. (2005) Evalulation of oxime efficacy in nerve agent poisoning: Development of a kinetic-based dynamic model, Toxicol. Appl. Pharmacol. 209, 193-202.

10. Peter, M.G. *Angew. Chem. Int. Ed. Engl.* **1989,** *28, 555.*

11. Veldhuyen, W.F.; Shallop, A. J.; Jones, R. A.; Rokita, S. E. *J. Am. Chem. Soc.* **2001**, *123,* 11126.

12. Modica, E.; Zanaletti, R.; Freccero, M.; Mela, M. *J. Org. Chem.* **2001**, *66,* 41.

13. Bakke, B. A.; McIntosh, M. C.; Turnbull, K. D. *J. Org. Chem.* **2005**, *70,* 4338-4345.

2. First Library

2.1 Introduction

An initial library of seven *para*-Quinone Methide Precursors (*p*-QMPs) (Figure 2.1) was produced during discussion with collaborators. These seven compounds use vanillin as a scaffold, where variations between them are the result of group substitutions at only the phenolic position. Compound E represents this base vanillin scaffold. For the amine leaving group, each QMP was held constant using dimethyl ammonium.

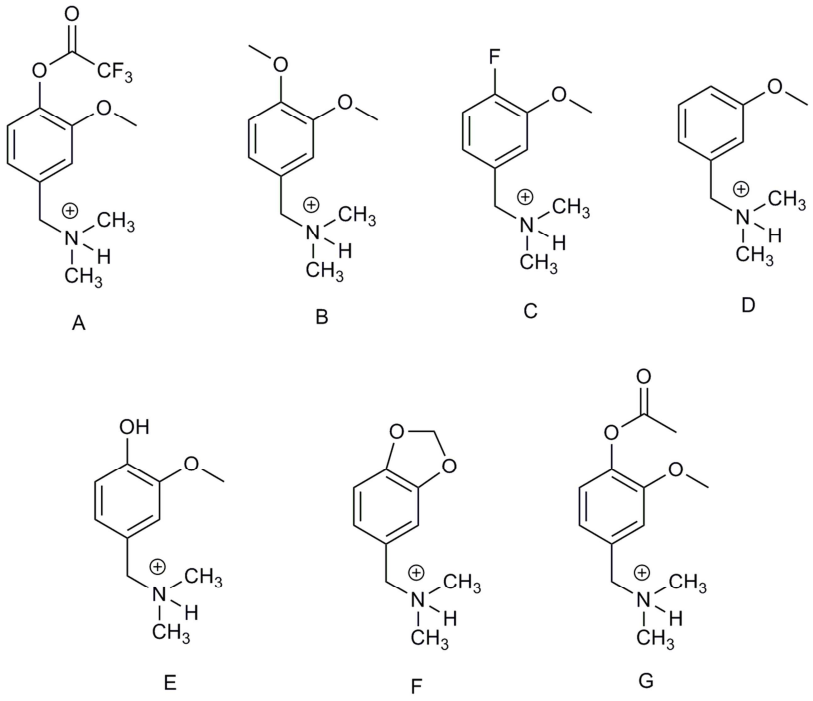

Figure 2.1: Initial Library of Quinone Methide Precursor Compounds

2.2 Preparation of Compounds for Molecular Docking

In order to dock these compounds into the active site of aged AChE, they first required preparation in order to provide meaningful results. Initially, all seven *p*-QMPs were built in GaussView 4.1.2[1]. Several different conformations of each compound were manually generated by altering bond angles and distances in order to give a best attempt at discovering each compound's global energy minimum. Then, all seven compounds and their alternate conformations were optimized with Gaussian 09[2] using the B3LYP/6-311+G** level of theory with a Polarizable Continuum Model[3] of Solvation of water. After the optimizations, the lowest energy conformation for each compound was determined and underwent vibrational frequency analysis at B3LYP/6-311+G** to look for the absence of imaginary frequencies, which would confirm that the geometry was a minimum on the potential energy surface. After confirmation of the absence of imaginary frequencies, then Merz-Kollman charge calculations were performed at the B3LYP/6-311+G** level of theory on each compound's lowest energy conformation to complete their preparation for molecular docking.

2.3 Molecular Docking

Molecular Docking is a computational technique that can give insight into the possible orientations of ligands inside receptors by examining the electrostatic interactions between the two. Typically, the ligand is treated as flexible with no rotational or torsional restrictions whereas the receptor is treated as rigid and no torsion or rotation is permitted. For this research, *p*-QMPs were docked inside the active site of thirteen snapshots of artificially aged human acetylcholinesterase (AChE). The thirteen artificially aged AChE snapshots (frames) were produced by Dr. Jeremy Beck as a portion of his dissertation.[4] The frames are stills taken from a 5 nanosecond molecular dynamics simulation of aged AChE with a generic QMP in the active site. The benefit of using these frames for our docking calculations is that induced fit effects on AChE from QMPs could be considered while still being able to treat AChE as rigid, which has a lower computational cost. Dr. Jeremy Beck sourced the structure of AChE from an available crystal structure in the Protein Data Bank (PDB id 1B41[5]). He removed waters, cofactors, and an associated fasciculin-II peptide using UCSF Chimera.[6] He then restored any missing residues using electric ray AChE homology (PDB id 1C2B[7]) and then added a phosphonate to the catalytic Serine-203 residue (Ser203) in order to produce human aged AChE.

For the molecular docking simulations on these seven compounds, all compounds were docked into each of the 13 receptor frames using Autodock 4.0.[8] A 50 x 50 x 50 $Å^3$ grid box was produced and centered at a moiety known as the oxyanion hole in order to limit the calculation to the active site and associated gorge to reduce computational expense. For each compound, 200 poses (snapshots of the compounds inside AChE) were generated for every receptor frame. This resulted in a total of 2600 poses per compound.

After completion of the molecular docking simulations, the positioning of these compounds within aged AChE was evaluated. Each docking simulation output contained 200 poses organized in a histogram from lowest binding energy to highest. The histogram associated poses with very similar binding energies into one bin. Each bin was examined and the distance measured for every pose within it. A bin with 75% or more of its poses falling into one of the three categories, which will be explained below had all of its poses designated as that category. This reduced the amount of manpower hours necessary to score each compound. Lastly, the poses associated with each category were summed and divided by the total number of poses per compound to give percentages.

Each pose was evaluated and classified into two categories: “within 3.7 Å” and “other”. A “within 3.7 Å” pose was considered to be one that had a distance equal or less than 3.7 Å between the *p*-QMP benzylic carbon and phosphonate oxygen on Ser203. An “other” pose covers any pose that has a benzylic carbon to phosphonate oxygen distance greater than 3.7 Å. A sub-category of “within 3.7 Å”, titled “within 3.7 Å, reactive orientation” was created to describe poses satisfying the distance requirement but also having the QMP’s amine leaving group oriented away from the phosphonylated serine oxygens. This orientation would result in minimal steric interference if the desired alkylation reaction were to occur via S_N2 direct displacement.

2.4 Molecular Docking Results

After completing the manual scoring process as outlined in Section 2.3, a table of the results was produced (Table 2.1).

Compound	Within 3.7 Å, reactive orientation (%)	Within 3.7 Å, unreactive orientation (%)	Other (%)
A	31.9	4.6	63.5
B	37.4	15.9	46.7
C	29.7	30.3	40
D	23.2	40.9	35.9
E	17.6	28.3	54.1
F	15.6	43.3	41.1
G	38.8	11.1	50.1

Table 2.1: Molecular Docking Results for First Library

Of these seven compounds, those with the highest proportion of poses within 3.7 Å were C, D, and F, which have fluorine, no functional, and acetal substitutions at the phenolic position, respectively. This was a rather interesting finding, as A, E, and G are the three worst performing compounds by this same metric and chemical intuition suggests that these compounds might preferentially undergo an S_N1 dissociation rather than a direct displacement reaction. Additionally, A, E, and G had the highest percentages of their poses exceeding 3.7 Å in distance between their benzylic carbons and the phosphonylated serine oxygens. Further experimental data regarding these ligands and enzyme itself would be ideal so that plausible, meaningful explanations of these trends are better supported. Therefore, Molecular Dynamics simulations

were performed on the library of seven compounds to simulate the interactions between the ligands and the aged AChE active site and obtain more information.

2.5 Molecular Dynamics (MD)

Molecular Dynamics is a computational method that permits one to simulate how a ligand might interact with a receptor or other molecule in a variety of solvents (or the gas phase) over time. In this calculation, both the ligand and the enzyme are treated as flexible, which permits a better approximation than molecular docking of what could be happening on an atomic level during experiments. For this application, the three lowest energy clusters from the previous molecular docking calculations were used as input geometry for the MD simulations. These input geometries placed the *p*-QMPs at varying distances from the phosphonylated serine residue within AChE's active site. All 13 prepared aged AChE receptor frames were used in these calculations, making a maximum total of 39 MD calculations per ligand. These were performed using the Sander module in AMBER11.[9] The simulated system was neutralized with Na^+ ions and solvated with explicit water. After this preparation, the simulated system underwent two minimizations. The first set of minimizations involved 500 steps of a calculation known as Steepest Descent Minimization[10], where the overall energy of the system is pushed away from any local maxima as quickly as possible while permitting the calculations to have larger error in their approximations. Next, the simulated system underwent 500 steps of a calculation known as Conjugate Gradient Minimization[10], which lowers the system's energy at a much slower rate so that it can be approximated with more accuracy. This allows the system to be brought closer to its global minimum. For the second set of minimizations, the system underwent another 1000 steps of Steepest Decent Minimization followed by 1500 steps of Conjugate Gradient Minimization. After these minimizations, the system was heated linearly from 0 Kelvin to 300 Kelvin over 20 picoseconds (10,000 steps of 2 femtoseconds) at 1 atm. After heating, MD

calculations were performed on this system over 1 nanosecond (500,000 steps of 2 femtoseconds).

After completion of the MD calculations, it became readily apparent that characterization of the enzyme AChE would be necessary in order to derive meaning from the results. For this characterization, the gorge to the active site of AChE was labeled based upon the distance between the phosphonate oxygens on Ser203 in the active site to certain residues in specific regions in the gorge (Table 2.2).

Zone	Distance from Ser203
Active Site (AS)	0 - 5 Å
Between AS and BN	5- 7 Å
Bottleneck (BN)	7 - 9.5 Å
Gorge Mouth (GM)	10 - 15 Å
Other	15 Å+

Table 2.2: AChE Zones (All bounds closed except “Between AS and BN” and “Other”)

2.6 Molecular Dynamics Results

Using the previously defined zones (Table 2.3), a table of results was produced by measuring the distance between the benzylic carbon of each QMP and the phosphonylated Serine oxygens in the active site for every still frame in the MD calculation (500 per 1ns MD). Every still frame was classified as one of the five zones. After every still frame was classified (using Excel → Filter) a fraction of the total number of still frames per ligand (typically 19500) was taken and a fraction of total poses present in a particular zone was then determined (Table 2.4).

Name	% Active Site	% Between AS and BN	% Bottleneck	% Gorge Mouth	% Other
A	47.5	18.5	11.9	20.0	20.7
B	44.3	22.6	9.2	22.2	24.3
C	46.6	16.3	10.6	24.5	18.2
D	45.8	27.2	7.1	18.1	29.0
E	44.7	23.2	6.0	22.6	26.7
F	58.2	12.9	10.4	16.6	14.8
G	49.8	10.9	14.2	20.7	15.3

Table 2.3: MD Results for First Library

Compound	Mean	Median	Mode	Max	Min
A	6.45	5.18	3.30	15.46	2.77
B	6.47	5.33	3.64	16.05	2.66
C	6.83	5.19	5.41	15.65	2.73
D	6.09	5.17	3.35	16.97	2.68
E	6.63	5.18	6.66	16.00	2.73
F	5.72	3.82	3.23	15.35	2.73
G	6.62	5.02	3.28	15.22	2.78

Table 2.4: MD Statistics Measuring Distance between Phosphonate Oxygen and QMP Benzylic Carbon for First Library

The 3 compounds with highest affinity for the active site after examining the MD results are A, F, and G. Compound F (acetal) also happens to be one of the best performers in the Molecular Docking studies. However, these MD results should be compared with Molecular

Docking results very carefully, as it is important to acknowledge that the upper boundary for the "active site" in MD is 5.0 Å, whereas that bound is 3.7 Å in Molecular Docking results.

Focusing back onto the MD results in Figure 2.4, a curious question is posed – why does Compound E (hydroxyl at the phenolic position) perform several percentage points lower than Compounds A and G, which should form the same QM intermediate if they undertake S_N2 dissociation? A closer look was taken at Compound E to suggest an explanation for the deviance.

2.7 Analysis of Compound E

In an attempt to understand the deviance from expected values, one MD video from each of the 13 receptor frames were viewed in an attempt to explain why this particular compound preferred to orient itself further away from the phosphonylated serine-203 residue (S203-OP adduct).

In most of the videos observed, the ligand (Compound E) was visualized interacting with Y124 and W86. Y124 is an aromatic residue (tyrosine) located in the Bottleneck zone. It is capable of hydrogen bond donation and acceptance, as well as cation-pi interactions. W86 is an aromatic residue (tryptophan) that is capable of only hydrogen bond acceptance and cation-pi interactions. Three labeled images (Figures 2.2, 2.3, and 2.4) are displayed below and explained.

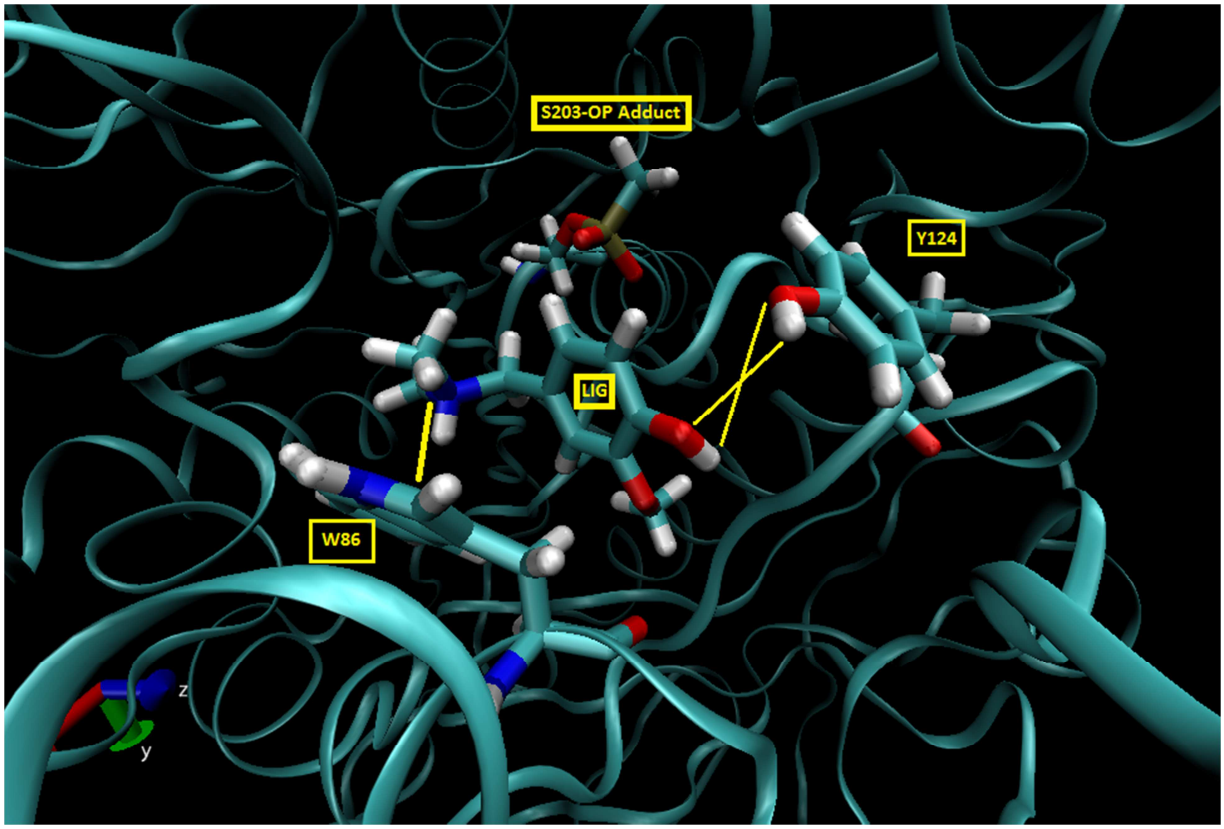

Figure 2.2: Compound E interacting with residues of interest within AChE

The first image (Figure 2.2) suggests that the ligand Compound E's hydroxyl group at the phenolic position may be involved in unique hydrogen bonding reciprocity with Y124 not demonstrated by the rest of the seven compounds. The image also suggests that cation-pi interactions between the dimethylammonium leaving group of the ligand and W86 may also play a role in tethering the ligand to residues outside of the upper bound for the active site. These residues and the suggested interactions are indicated in yellow.

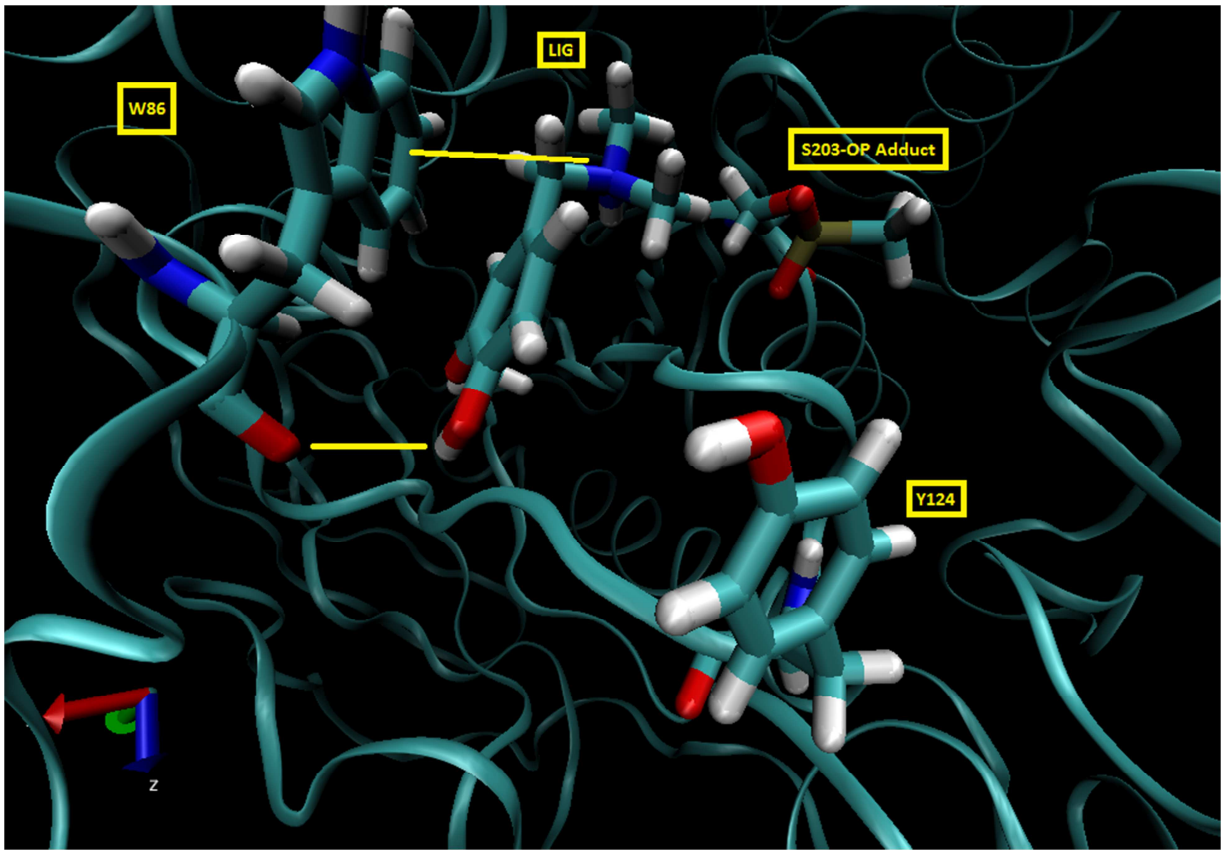

Figure 2.3: A second view of Compound E interacting with residues of interest within AChE

The second image (Figure 2.3) above does not show interactions between the ligand and Y124. However, it does imply hydrogen bond donation and cation-pi interactions between the ligand and W86.

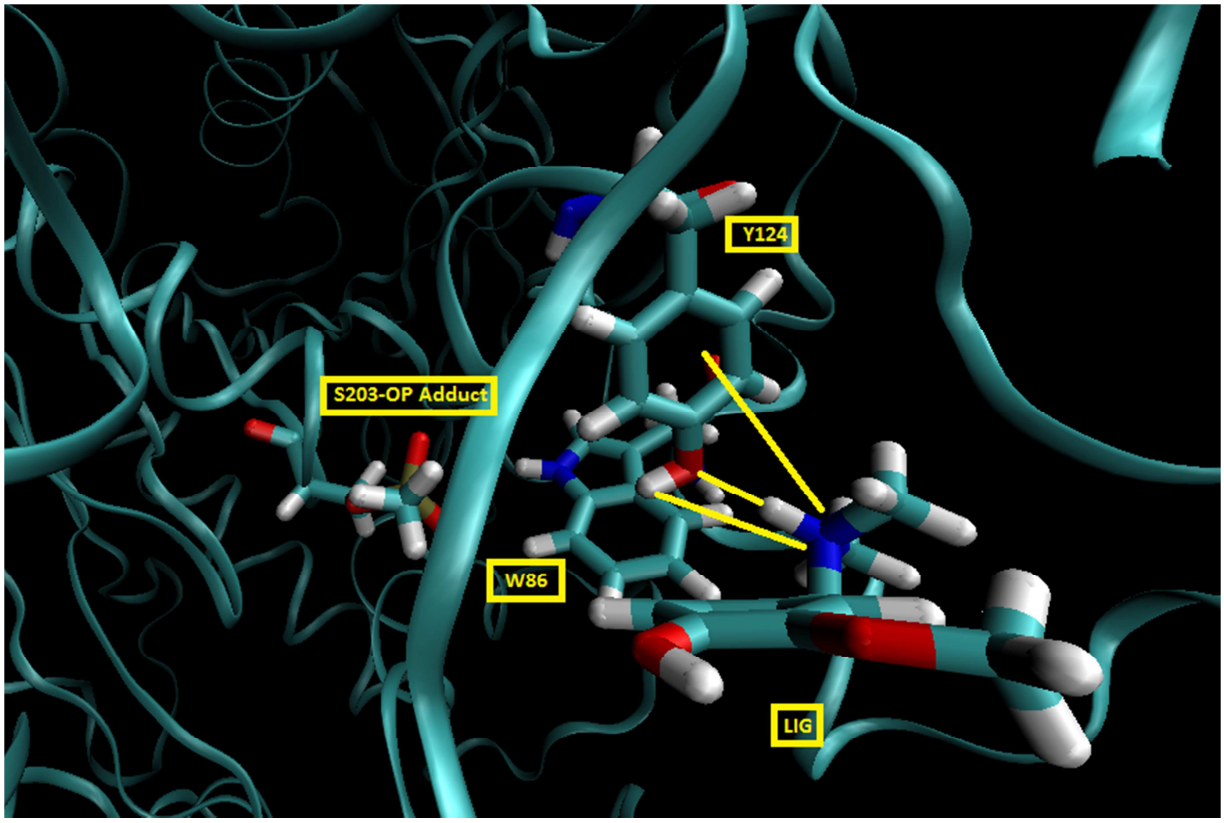

Figure 2.4: A third view of Compound E interacting with residues of interest within AChE

The third view (Figure 2.7) suggests that hydrogen bonding reciprocity between Y124 and the ligand are present, as well as the implication of potential cation-pi interactions with Y124 from the ligand. In this third image, there are no interactions with W86.

These three images highlight three different orientations of Compound E near AChE's gorge bottleneck. They represent the majority of Compound E's simulated interactions with the enzyme. The most plausible explanation of Compound E's inferior performance in comparison to Compounds A and G is that the presence of a hydroxyl group at the phenolic position on Compound E allows it to both donate and accept hydrogen bonding with Y124. In combination with its protonated dimethylammonium leaving group permitting cation-pi interactions with residues near the active site, this added hydrogen bond acceptance-donor reciprocity uniquely

enables Compound E to select Y124 and reduce the amount of time it spends within the active site zone.

2.8 References

1. GaussView, Version 4.1.2, Dennington, Roy; Keith, Todd; Millam, John. Semichem Inc., Shawnee Mission, KS, 2009.

2. Gaussian 09, Revision D.01, Frisch, M. J.; Trucks, G. W.; Schlegel, H. B.; Scuseria, G. E.; Robb, M. A.; Cheeseman, J. R.; Scalmani, G.; Barone, V.; Mennucci, B.; Petersson, G. A.; Nakatsuji, H.; Caricato, M.; Li, X.; Hratchian, H. P.; Izmaylov, A. F.; Bloino, J.; Zheng, G.; Sonnenberg, J. L.; Hada, M.; Ehara, M.; Toyota, K.; Fukuda, R.; Hasegawa, J.; Ishida, M.; Nakajima, T.; Honda, Y.; Kitao, O.; Nakai, H.; Vreven, T.; Montgomery, J. A., Jr.; Peralta, J. E.; Ogliaro, F.; Bearpark, M.; Heyd, J. J.; Brothers, E.; Kudin, K. N.; Staroverov, V. N.; Kobayashi, R.; Normand, J.; Raghavachari, K.; Rendell, A.; Burant, J. C.; Iyengar, S. S.; Tomasi, J.; Cossi, M.; Rega, N.; Millam, N. J.; Klene, M.; Knox, J. E.; Cross, J. B.; Bakken, V.; Adamo, C.; Jaramillo, J.; Gomperts, R.; Stratmann, R. E.; Yazyev, O.; Austin, A. J.; Cammi, R.; Pomelli, C.; Ochterski, J. W.; Martin, R. L.; Morokuma, K.; Zakrzewski, V. G.; Voth, G. A.; Salvador, P.; Dannenberg, J. J.; Dapprich, S.; Daniels, A. D.; Farkas, Ö.; Foresman, J. B.; Ortiz, J. V.; Cioslowski, J.; Fox, D. J. Gaussian, Inc., Wallingford CT, 2009.

3. Mennucci, B. (2012), Polarizable continuum model. WIREs Comput Mol Sci, 2: 386–404. doi: 10.1002/wcms.1086

4. Beck, J. M., Ph.D. Dissertation, The Ohio State University, 2011.

5. Kryger, G.; Harel, M.; Giles, K.; Toker, L.; Velan, B.; Lazar, A.; Kronman, C.; Barak, D.; Ariel, N.; Shafferman, A.; Silman, I.; Sussman, J. L.Acta Crystallogr., Sect. D 2000, 56, 1385-1394

6. Pettersen, E. F.; Goddard, T. D.; Huang, C. C.; Couch, G. S.; Greenblatt, D. M.; Meng, E. C.; Ferrin, T. E. J. Comput. Chem. **2004**, *25*, 1605-1612.

7. Bourne, Y.; Grassi, J.; Bougis, P. E.; Marchot, J. J. Biol. Chem. **1999**, *274*, 30370-30376

8. Morris, G. M., Huey, R., Lindstrom, W., Sanner, M. F., Belew, R. K., Goodsell, D. S. and Olson, A. J. (2009) Autodock4 and AutoDockTools4: automated docking with selective receptor flexiblity. J. Computational Chemistry **2009**, *16*: 2785-91.

9. Case, D. A.; Darden, T. A.; Cheatham, T. E., III; Simmerling, C. L.; Wang, J.; Duke, R. E.; Luo, R.; Crowley, M.; Walker, R. C.; Zhang, W.; Merz, K. M.; Wang, B.; Hayik, S.; Roitberg, A.; Seabra, G.; Kolossváry, I.; Wong, K. F.; Paesani, F.; Vanicek, J.; Wu, X.; Brozell, S. R.; Steinbrecher, T.; Gohlke, H.; Yang, L.; Tan, C.; Mongan, J.; Hornak, V.; Cui, G.; Mathews, D. H.; Seetin, M.G.; Sagui, C.; Babin, V.; Kollman, P. A. AMBER 11, University of California, San Francisco, 2008.

10. Adcock, S. A., & McCammon, J. A. Molecular Dynamics: Survey of Methods for Simulating the Activity of Proteins. *Chemical Reviews* **2006**, *106*(5), 1589–1615. doi:10.1021/cr040426m

3. Second Library

3.1 Introduction

After examination of the MD data shown in the previous chapter, three compounds with the highest affinity for the active site were selected as scaffolds to produce a new library of compounds to evaluate. An additional six compounds were selected from MD calculations performed by fellow undergraduates Keegan Fitzpatrick and Andrew Franjesevic on the same basis. Based on their origins, one letter codes were assigned to each compound to produce three "classes" of QMPs – T, A, and K (Figure 3.1).[1]

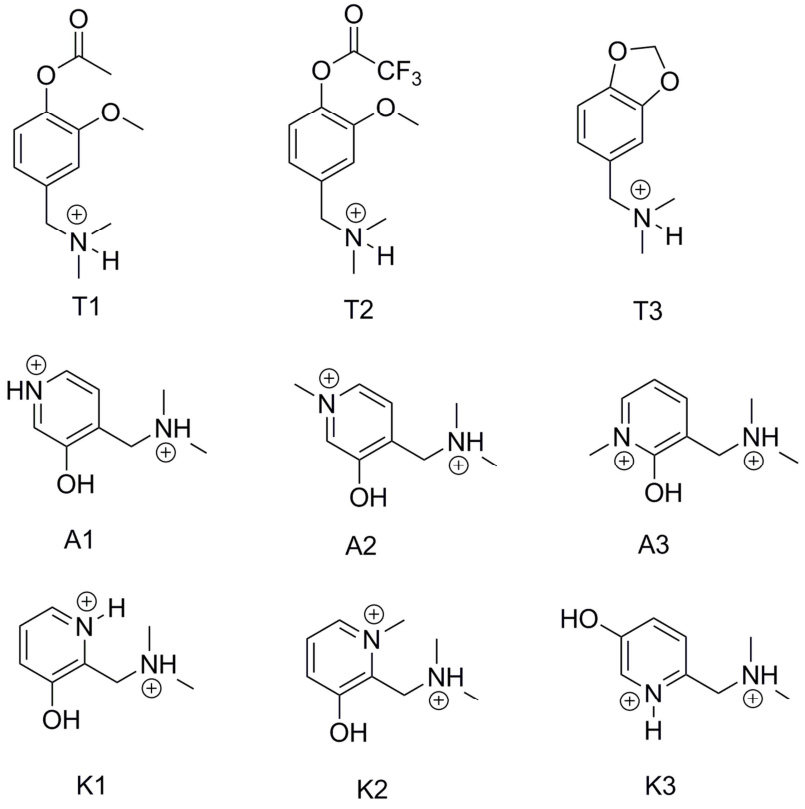

Figure 3.1: QMP Structures used as base scaffolds for an expanded library of new variants.

After discussion with collaborators, two variations in the base scaffolds evaluated for their effects on active site affinity. The first variation was a substitution of the amine leaving group, substituting dimethylammonium with dimethylammonia, pyrrolidine, piperidine, or morpholine functionals. The second variation was a change in the protonation state of the leaving group and heterocyclic nitrogen (if applicable) to neutral, protonated, or methylated analogs. Using these variations, ninety-nine analogs were designed. From those, seventy-eight were selected for evaluation (Figure 3.2, 3.3, 3.4, 3.5) using the molecular docking and molecular dynamics procedures described in Chapter 2. The remaining compounds were given to fellow undergraduates to perform the same calculations.

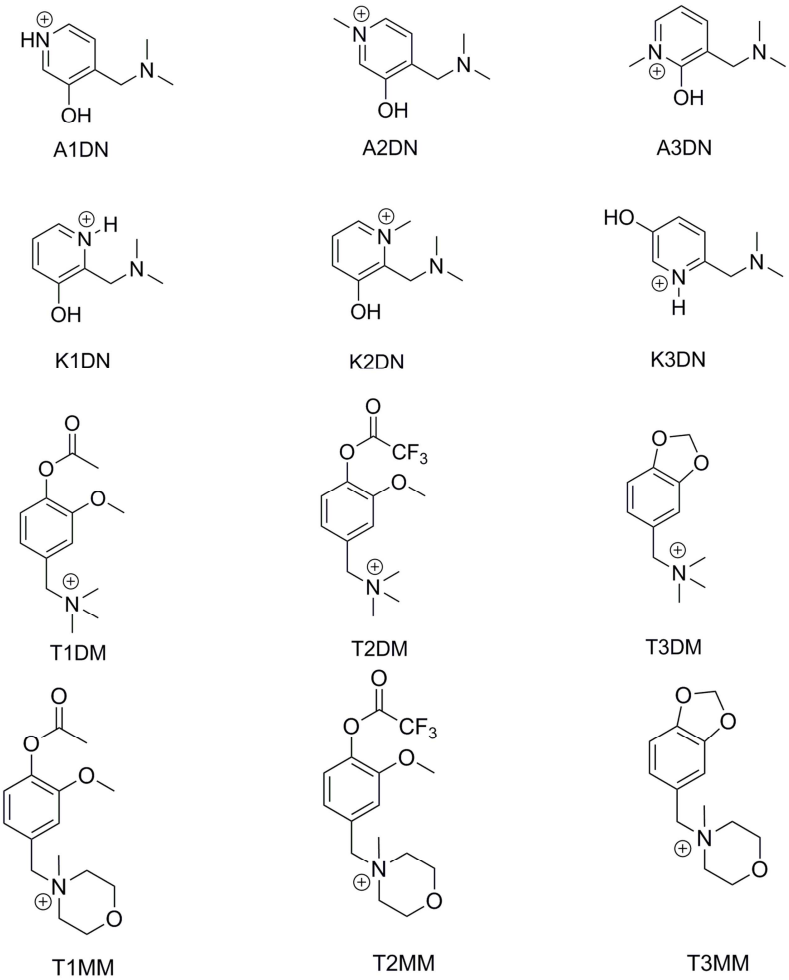

Figure 3.2: Second Library of Compounds

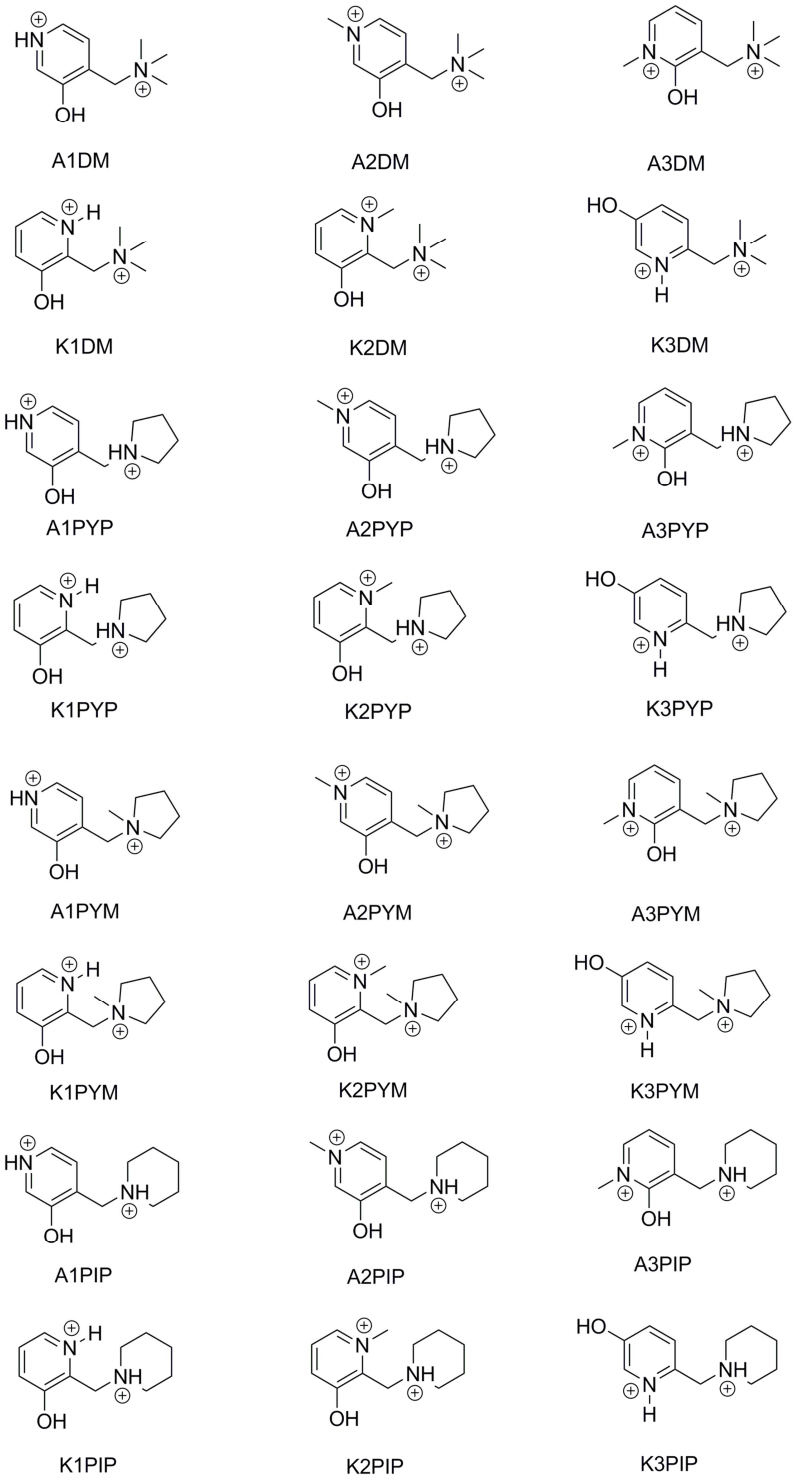

Figure 3.3: Second Library of Compounds

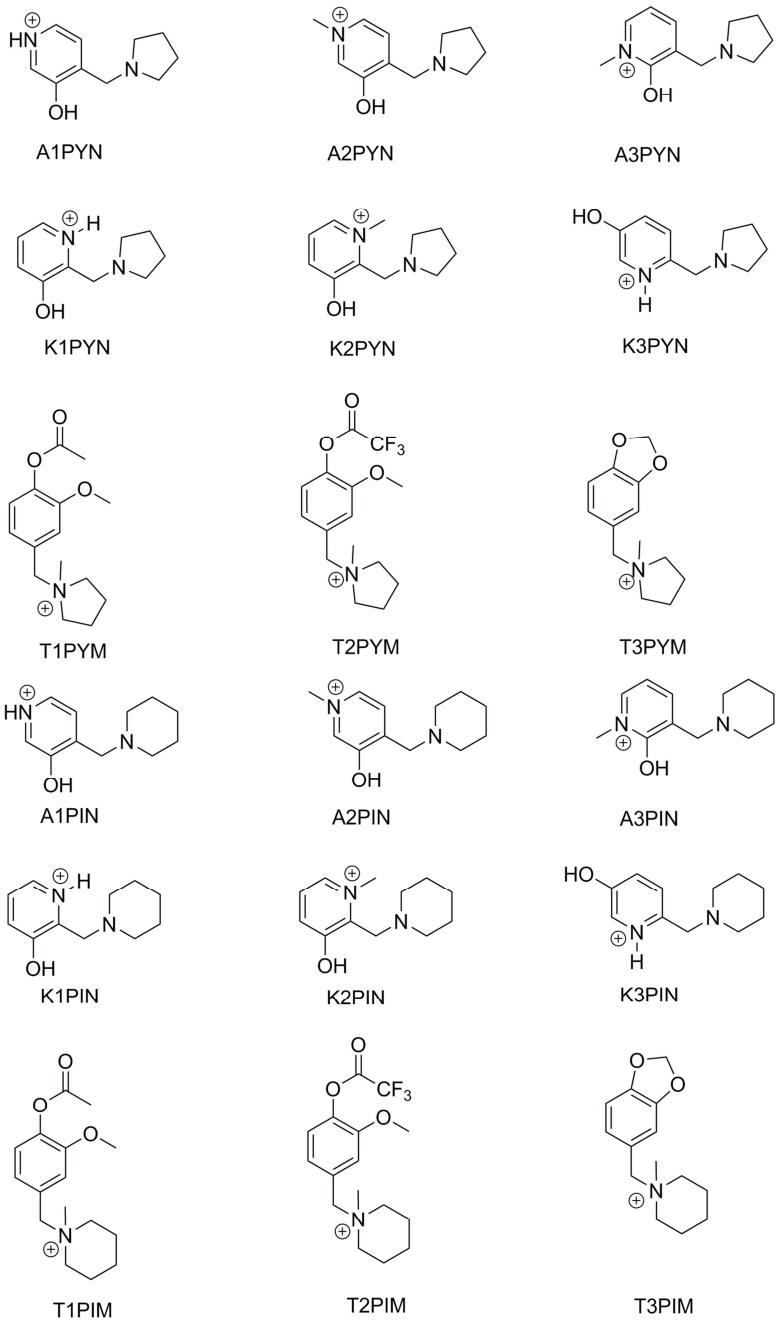

Figure 3.4: Second Library of Compounds

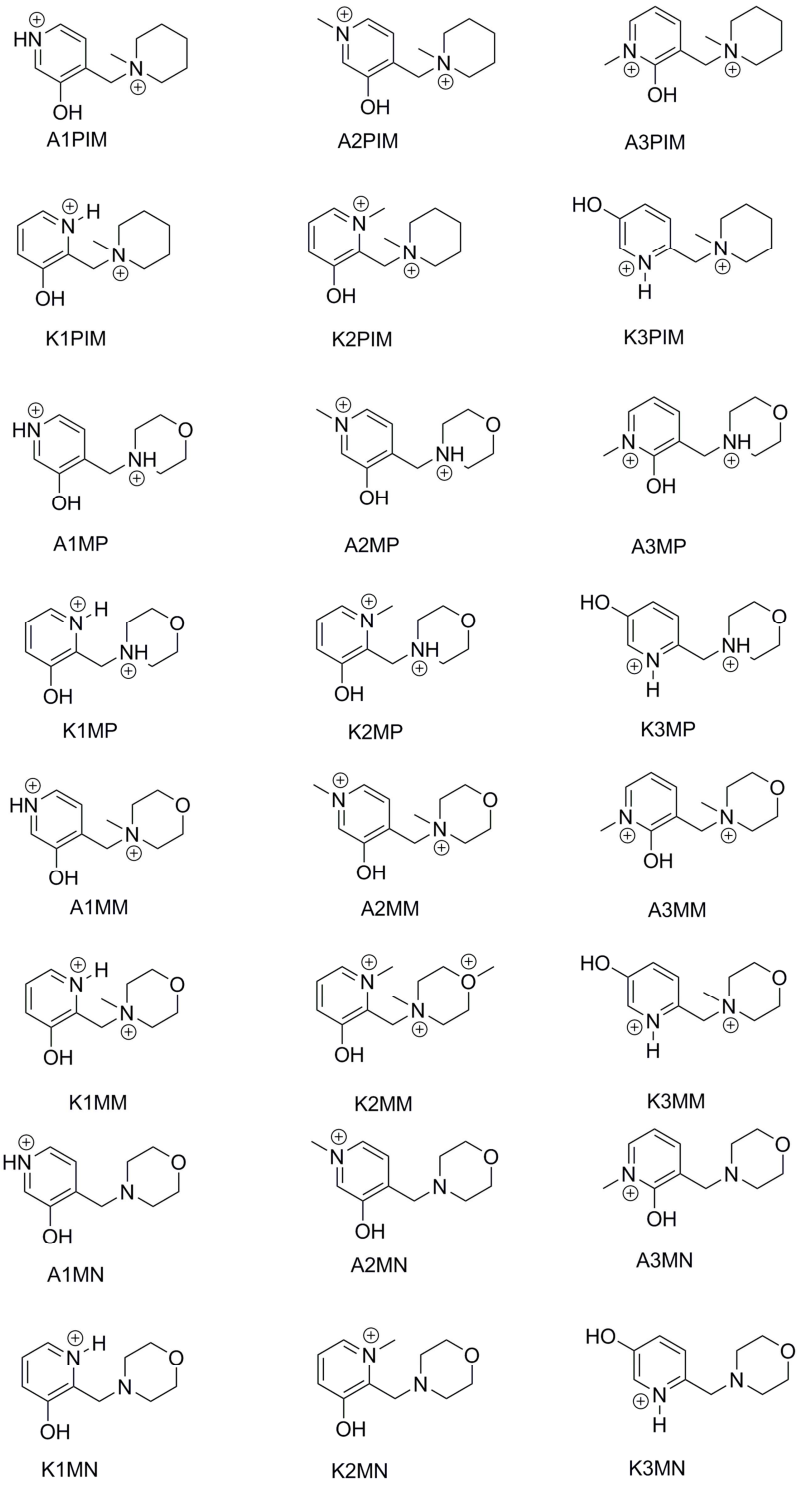

Figure 3.5: Second Library of Compounds

The naming scheme for this library is relatively straightforward. As mentioned earlier in this chapter, the first two characters in the name indicate the class that the scaffold belongs to, and which specific scaffold was used. The remaining characters indicate which amine leaving group is present on the compound, followed by what the protonation state of the compound is. For leaving groups, dimethylammonia is indicated by D, pyrrolidine is indicated by PY, piperidine by PI, and morpholine by M. For protonation states, neutral is indicated by N, protonated by P, and methylated by M. The order of the codes is the same for every compound in this library.

3.2 Molecular Dynamics Results

Using the same zoning criteria from the previous chapter, tables of results were produced from the MD calculations (Table 3.1).

Compound Name	% Active Site	% Between AS and BN	% Bottleneck	% Gorge Mouth	% Other
A1DN	20.88	35.66	26.87	11.95	4.65
A1MN	21.31	32.82	30.84	12.32	2.72
A1PIN	27.06	38.07	24.28	9.05	1.55
A1PYN	37.10	31.64	22.59	5.23	3.45
A2DN	36.77	25.85	18.70	13.95	4.73
A2MN	9.12	29.42	22.55	33.19	5.71
A2PIN	25.71	46.33	15.36	10.69	1.90
A2PYN	30.37	40.46	20.32	6.39	2.45
A3DN	40.58	27.17	23.42	7.01	1.82
A3MN	11.68	42.33	25.32	17.29	3.38
A3PIN	27.01	34.93	27.32	9.42	1.33
A3PYN	30.39	31.36	28.09	9.23	0.93
A1DM	37.54	32.41	7.22	17.64	5.20
A1MM	45.72	15.71	2.74	30.65	5.17
A1MP	41.15	23.10	5.49	25.79	4.48
A1PIM	53.88	14.54	1.59	27.21	2.78
A1PIP	67.66	14.06	2.78	8.20	7.30
A1PYM	45.54	23.09	5.28	17.39	8.70
A1PYP	65.76	16.43	1.76	9.59	6.46
A2DM	61.47	10.11	5.42	14.83	8.17
A2MM	21.48	36.23	11.69	25.11	5.49
A2MP	49.66	16.47	7.37	20.21	6.29
A2PIM	23.84	42.04	8.49	22.29	3.35
A2PIP	57.36	21.55	7.86	7.04	6.18
A2PYM	41.59	32.70	5.47	14.41	5.83
A2PYP	62.85	17.58	1.95	13.38	4.24
A3DM	73.75	5.21	3.53	13.46	4.05
A3MM	24.64	18.00	9.15	39.31	8.89
A3MP	40.97	15.79	9.92	28.71	4.60
A3PIM	64.57	7.18	5.87	17.98	4.39
A3PIP	68.51	6.51	4.83	15.31	4.85

Compound Name	% Active Site	% Between AS and BN	% Bottleneck	% Gorge Mouth	% Other
A1DM	37.54	32.41	7.22	17.64	5.20
A1MM	45.72	15.71	2.74	30.65	5.17
K1DN	44.44	23.06	16.73	10.52	5.25
K1MN	28.85	41.55	16.21	9.14	4.25
K1PIN	49.81	29.08	13.66	5.88	1.57
K1PYN	41.57	33.18	15.70	8.22	1.33
K2DN	29.86	25.24	21.72	17.98	5.20
K2MN	24.16	29.72	20.76	21.82	3.53
K2PIN	38.46	17.23	22.88	15.38	6.05
K2PYN	34.83	32.55	16.02	12.76	3.85
K3DN	34.32	22.46	34.33	6.82	2.07
K3MN	17.82	34.34	25.76	16.90	5.18
K3PIN	16.56	29.96	30.23	19.81	3.45
K3PYN	25.36	30.37	31.24	10.87	2.16
K1DM	63.06	7.36	2.48	16.23	10.87
K1MM	36.54	17.38	2.66	37.17	6.24
K1MP	53.95	12.46	7.29	16.71	9.59
K1PIM	58.09	9.74	4.60	22.63	4.94
K1PIP	56.53	17.83	4.93	16.76	3.94
K1PYM	71.29	5.65	2.43	18.26	2.37
K1PYP	68.65	10.57	2.00	15.33	3.45
K2DM	42.06	20.92	5.51	21.01	10.51
K2MM	44.92	18.35	1.93	28.52	6.28
K2MP	40.17	14.75	3.41	27.74	13.93
K2PIM	44.93	17.86	9.48	24.45	3.28
K2PIP	67.17	8.26	4.04	15.23	5.31
K2PYM	65.86	12.62	3.43	16.08	2.02
K2PYP	56.40	9.46	6.00	23.10	5.04
K3DM	55.48	15.09	6.81	18.42	4.21
K3MM	35.37	12.06	7.23	37.23	8.11
K3MP	42.07	18.10	0.78	28.78	10.27
K3PIM	46.40	14.62	6.62	27.97	4.39
K3PIP	56.53	8.39	3.68	15.76	15.63
K3PYM	55.61	15.35	5.64	20.27	3.14
K3PYP	64.69	15.78	4.70	9.04	5.78

Compound Name	% Active Site	% Between AS and BN	% Bottleneck	% Gorge Mouth	% Other
T1DM	50.4	14.1	11.0	20.7	3.8
T1MM	25.7	18.1	23.2	29.0	4.0
T1PIM	47.5	21.9	9.8	18.1	2.8
T1PYM	44.3	11.6	18.2	23.8	2.0
T2DM	51.7	8.3	12.3	20.9	6.9
T2MM	25.4	15.2	25.0	31.3	3.2
T2PIM	49.7	11.7	15.5	20.5	2.6
T2PYM	54.7	20.5	9.3	13.8	1.7
T3DM	63.2	9.5	8.5	14.2	4.5
T3MM	30.0	11.9	19.6	34.0	4.5
T3PIM	49.1	28.1	6.2	14.2	2.4
T3PYM	35.3	36.2	6.9	17.8	3.8

Table 3.1: MD Results for Second Library

Of these seventy-eight compounds, ten compounds with the highest and lowest affinities for the active site were identified, and their data was assimilated (Figure 3.3, Table 3.2, Figure 3.4, Table 3.3).

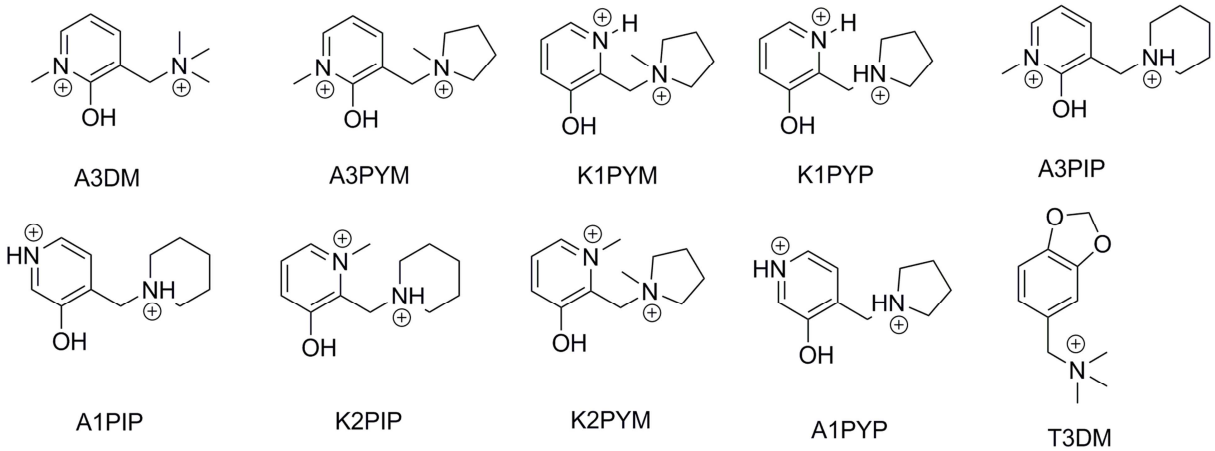

Figure 3.6: Compounds with highest active site affinity

Compound Name	% Active Site	% Between AS and BN	% Bottleneck	% Gorge Mouth	% Other
A3DM	73.70	5.20	3.50	13.50	4.10
A3PYM	71.40	4.60	1.90	17.60	4.50
K1PYM	71.30	5.70	2.40	18.30	2.40
K1PYP	68.60	10.60	2.00	15.30	3.50
A3PIP	68.50	6.50	4.80	15.30	4.80
A1PIP	67.70	14.10	2.80	8.20	7.30
K2PIP	67.20	8.30	4.00	15.20	5.30
K2PYM	65.90	12.60	3.40	16.10	2.00
A1PYP	65.80	16.40	1.80	9.60	6.50
T3DM	63.20	9.50	8.50	14.20	4.50

Table 3.2: MD results for compounds with highest active site affinity (high to low)

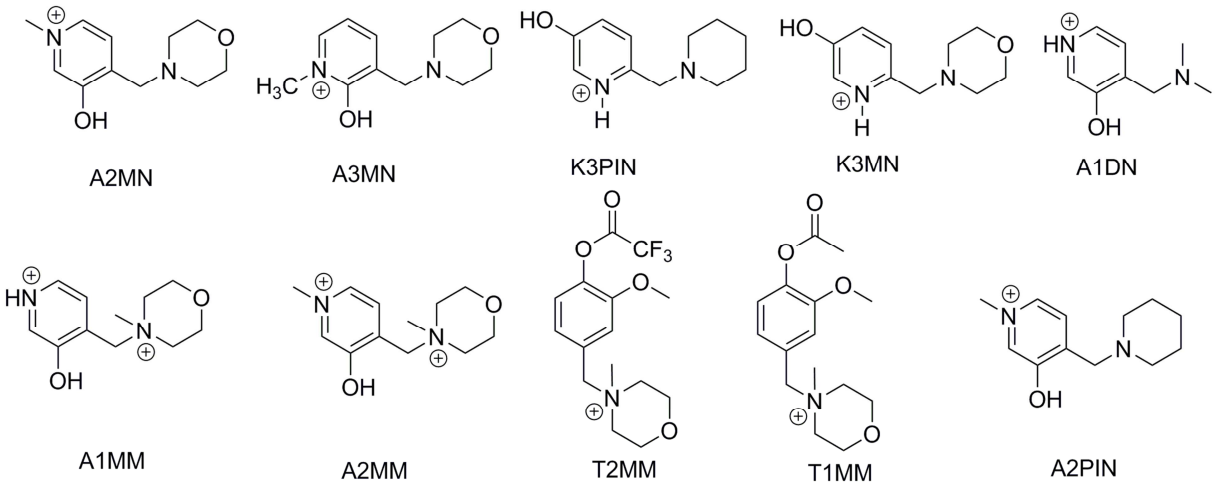

Figure 3.7: Compounds with lowest active site affinity

Compound Name	% Active Site	% Between AS and BN	% Bottleneck	% Gorge Mouth	% Other
A2MN	9.12	29.42	22.55	33.19	5.71
A3MN	11.68	42.33	25.32	17.29	3.38
K3PIN	16.60	30.00	30.20	19.80	3.40
K3MN	17.80	34.30	25.80	16.90	5.20
A1DN	20.88	35.66	26.87	11.95	4.65
A1MN	21.31	32.82	30.84	12.32	2.72
A2MM	21.50	36.20	11.70	25.10	5.50
T2MM	25.40	15.20	25.00	31.30	3.20
T1MM	25.73	18.06	23.22	28.99	4.00
A2PIN	25.71	46.33	15.36	10.69	1.91

Table 3.3: MD results for compounds with lowest active site affinity (low to high)

Comparing the ten compounds with highest active site affinity, it is readily apparent that the majority of these compounds had pyrrolidine and piperidine leaving groups. In fact, the only leaving group that did not have any representation in the top ten was morpholine. All but one of the top performers had pyridinium or methylpyridinium cyclic units, with the compound falling into tenth place containing a phenyl ring. Additionally, all but one of the top performers had protonation states of +2 with a 5-to-4 split of methylation to protonation.

Looking at the ten compounds with the lowest active site affinity of the library, seven of the ten compounds had morpholine leaving groups, suggesting that morpholine's absence from the highest affinity list is likely not a coincidence. Additionally, nine of the ten compounds had protonation states of +1. Most of these compounds have pyridinium or methylpyridinium rings, with a slightly larger proportion of the phenyl ringed vanillin compounds being present in this short list.

3.3 References

1. Fitzpatrick, Keegan. Computational Insights into the Alkylation Reactions of Pyridine and Pyridinium Quinone Methide Precursors: Studies Towards the Realkylation of Aged Acetylcholinesterase. Thesis, The Ohio State University, 2013.

4. Conclusions and Future Work

4.1 Conclusions

The data shows that the best performing leaving groups from the expanded library of seventy-eight were pyrrolidine and piperidine functional groups that also were protonated or methylated at the heterocyclic nitrogen. After observing MD simulation videos of these compounds, it was seen that because of the size of these leaving groups, they were not as close to W86 as the library of 7 dimethylammonium leaving group compounds were as discussed in Chapter 2 (Figure 4.1). While these larger leaving groups were still close enough to undergo cation-pi interactions, it appears that the conformation of those leaving groups prevented them from being flatter and therefore sitting closer to W86 (Figure 4.2). This inability to sit closely resulted in the benzylic carbon being closer in proximity to the Ser203 phosphonate oxygens, resulting in these compounds having better rankings.

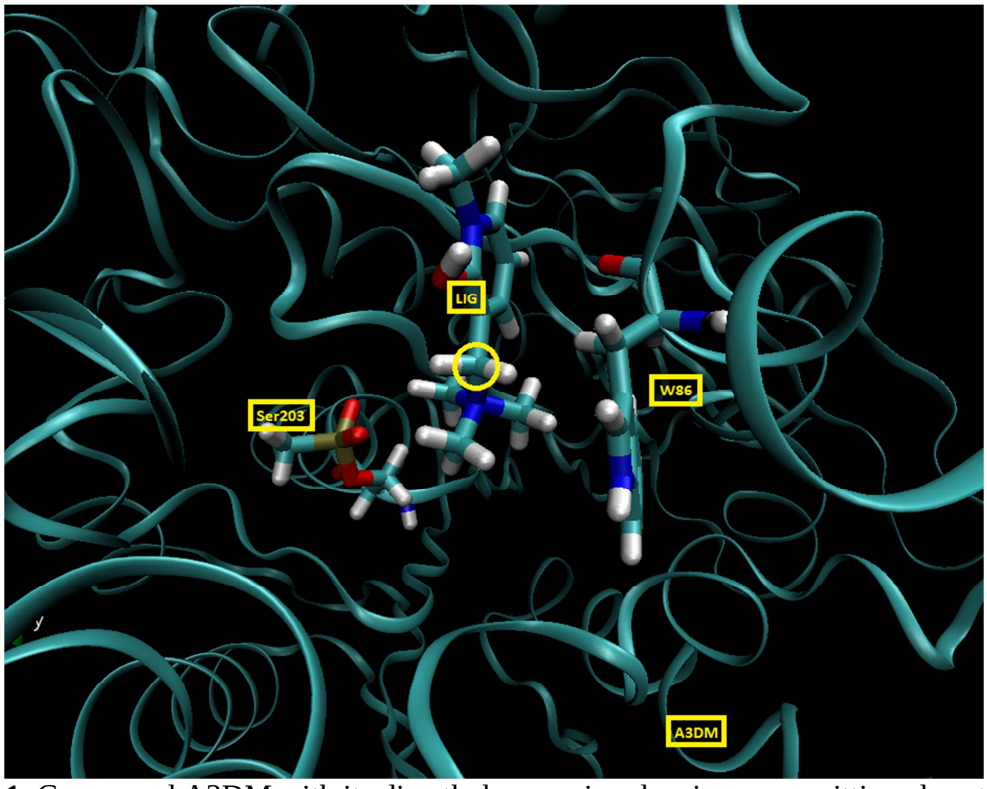

Figure 4.1: Compound A3DM with its dimethylammonium leaving group sitting close to W86.

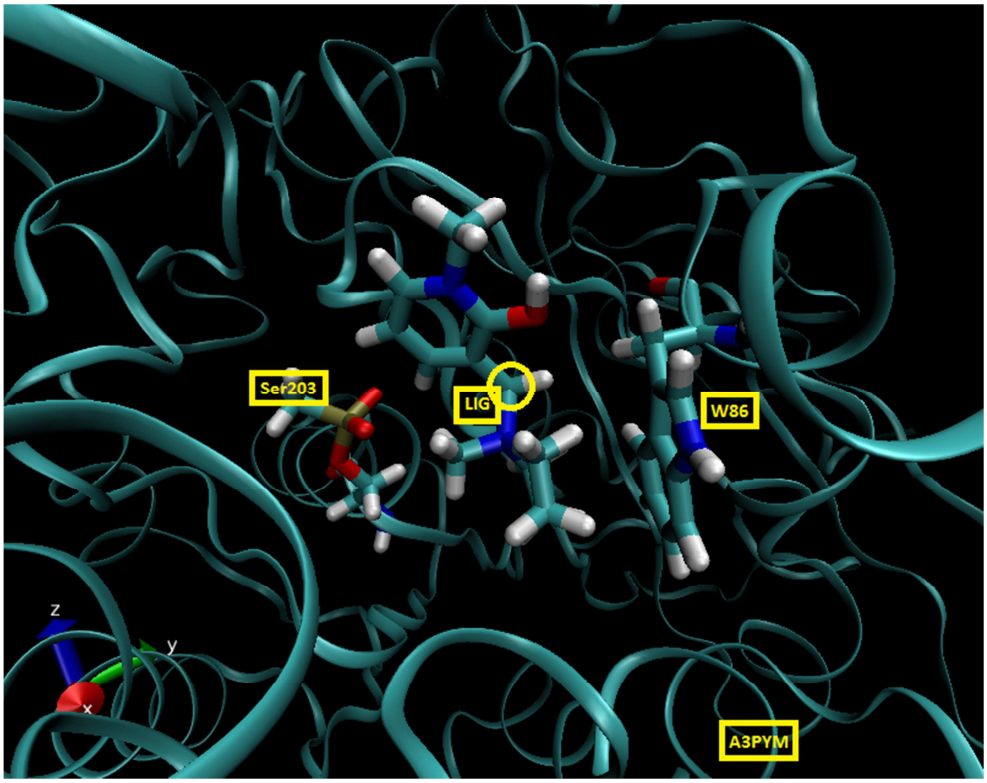

Figure 4.2: Compound A3PYM with its pyrrolidine leaving group sitting further from W86 and closer to Ser203.

Additionally, it was found that having a +2 protonation state increased the probability that compounds would be among those with the most affinity for the active site. Having a protonated leaving group aids in anchoring the QMPs to W86 in the Cation Binding Pocket (CBP), bringing the QMP within 4-7 Angstroms of the Ser203 residue on a regular basis. However, it seems that because of the ortho and para orientations of the protonated or methylated heterocyclic nitrogen of the pyridinium cyclic units, these compounds are particularly suited to interact with W86 and Y124 to minimize their benzylic carbon's distance to Ser203 over the source of an MD simulation (Figure 4.3). With less charged QMPs, they would typically bounce around within 3-6 Angstroms of their initial distance although sometimes movement between all 3 zones could be visualized. With these +2 protonation state QMPs, the QMPs themselves bounced around 2-3 Angstroms of their original distance. It seems that having that additional

charge in the ring permits H-bond acceptance from Y124 as well as alternating cation-pi interactions between the protonated leaving group and the pyridinium unit, reducing the distance that these compounds will move when they are in the active site.

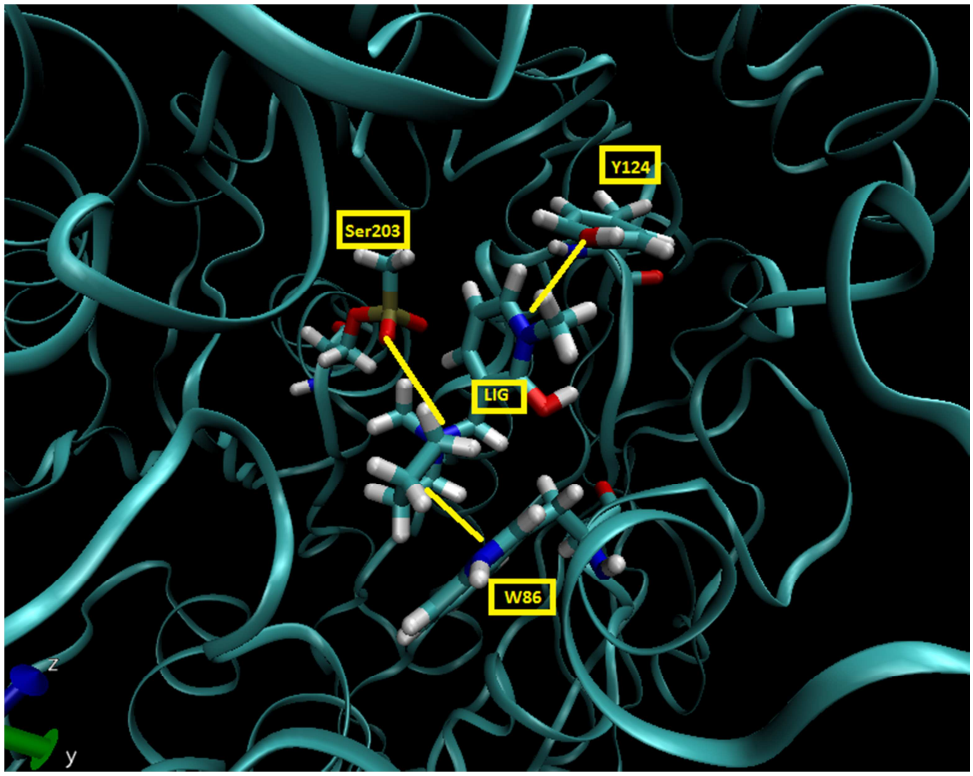

Figure 4.3: An illustration of the interactions between a +2 Protonation State Methylpyridinium QMP and W86, Y124, and Ser203.

Regarding the compounds with the lowest active site affinity, a +1 protonation state and a morpholine leaving group were the most commonly observed variations. A compound that has only a protonated amine leaving group, using the hypothesis suggested above, should have more variance when interacting with W86 in the CBP. For one of the worst performing compounds A3MN, interactions with residues in the bottleneck zone were commonly observed (Figure 4.4). Seemingly, an unprotonated amine leaving group may result in having the compounds “hang up” in the bottleneck . Regarding the morpholine leaving group performing poorly, it appears the

presence of the heterocyclic oxygen in the morpholine leaving group permits interactions with Y124, which are demonstrated by these compounds having such a high proportion of their still poses between the active site and the bottleneck.

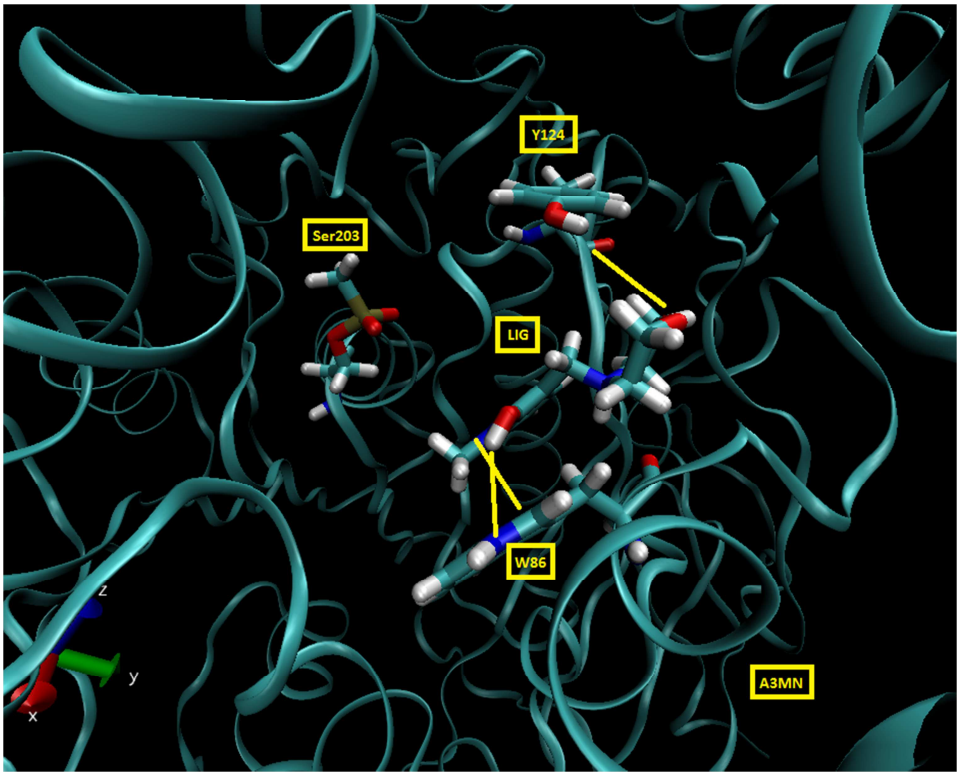

Figure 4.4: Compound A3MN, its unprotonated leaving group, and identification of interactions which might facilitate its poor affinity for the active site.

4.2 Future Work

With this larger library, we have shown the tunability of these molecules with regard to their affinity for the aged AChE active site. At this point, these results should be passed along to our experimental collaborators to focus their synthesis on QMPs with the structural characteristics that make binding possible. Additionally, the exploration of other scaffolds, namely quinolone and isoquinoline, should be considered.

Additionally, QM/MM calculations should be performed on some select QMPs in the active site of AChE to determine whether a quinone methide or an intermediate can be generated there. This is of significant importance to the project, as all of the computational work thus far has been associated with designing QMPs to be specific for the active site and evaluating the energetics of QMPs. Starting with QM/MM calculations is part of a progression towards determining the actual mechanism of alkylation and beginning design efforts relating to alkylation.